J. Physiol. (1981), **317**, *pp.* 317–334
With 9 text-figures
Printed in Great Britain

SINGLE PHOTON SIGNALS IN FLY PHOTORECEPTORS AND FIRST ORDER INTERNEURONES AT BEHAVIOURAL THRESHOLD

BY A. DUBS*, S. B. LAUGHLIN* AND M. V. SRINIVASAN*†

From the Departments of Neurobiology and Applied Mathematics†, Australian National University, P.O. Box 475, Canberra City, A.C.T. 2601, Australia*

(*Received 11 September 1980*)

SUMMARY

1. The contrast sensitivity of the optomotor response of the fly *Musca domestica* was measured using a moving sinusoidal grating as the stimulus. In parallel experiments intracellular recordings were made from photoreceptors and first order visual interneurones to determine their responses to the same threshold stimuli. Measurements of the spatial modulation transfer function for photoreceptors confirm that the optics of the eye were intact during recordings.

2. At the lowest intensity at which one can obtain an optomotor response, the photoreceptor signal is a train of discrete depolarizations, or bumps. With constant intensity stimuli, the temporal distribution of bumps follows the Poisson distribution with a mean rate proportional to luminance. The mean bump rate at the threshold intensity for a behavioural response is $1{\cdot}7 \pm 0{\cdot}7$ s^{-1} (mean $\pm$ S.D., $n = 25$).

3. Calibrations and the statistical properties of the bump train indicate that a bump represents one effective photon, implying that the bump: photon ratios are quantum capture efficiencies.

4. At low intensities the first order interneurones (the large monopolar cells or LMCs) show hyperpolarizing bumps each triggered by a receptor bump. Using a point source stimulus, centred in the field of view, the LMC bump rate is six times that in a single receptor viewing the same stimulus, as expected from the known projection of six receptor axons to each LMC. When using an extended stimulus (the grating), the bump rate is 18–20 times that in receptors. Comparison with earlier work suggests that this increased lateral summation of receptor inputs to LMCs only occurs at very low intensities.

5. In both receptors and LMCs the amplitudes and wave forms of bumps depend upon the position of a point source stimulus within the field of view. With the light in the periphery of the field the bumps are smaller and slower than when the light is in the centre. This difference in response suggests that spatial summation is brought about by lateral interactions, possibly between receptors.

6. At higher mean intensities the signal-to-noise ratios in receptors responding to the appropriate threshold stimuli increase with intensity. This is suggestive of a decrease in the extent of spatial and/or temporal summation in the optomotor pathway.

INTRODUCTION

To understand the function of the receptors and interneurones of a visual system, their responses must be placed within the context of the visual system's ability to make sensory discriminations, as judged from behavioural evidence. For example, we would have little appreciation of a receptor's spectral sensitivity if we were unaware that the animal in question possessed colour vision.

Our primary interest is in the ways that photon absorption, transduction and synaptic transfer in the peripheral visual system can limit visual acuity, and in the processing strategies that might be used to minimise any deleterious effects associated with these stages. The fly's visual system is particularly suitable for correlating receptor or interneuronal responses with behavioural thresholds (Reichardt, 1970). Both the optics and neuroanatomy of the visual system are well described (Kirschfeld, 1973; Strausfeld, 1976*a*, *b*), intracellular recordings have been made from anatomically identified photoreceptors and first, second and third order visual interneurones (Hardie, 1979; Zettler & Järvilehto, 1973; DeVoe & Ockleford, 1976; Dvorak, Bishop & Eckert, 1975; Hausen, 1976), while the fly's visual behaviour, and in particular the optomotor, tracking and fixation responses, have been analysed quantitatively (Reichardt, 1970; Land, 1977). Furthermore simple operative techniques allow the recording from an essentially intact retina, located in an animal performing its normal respiratory and circulatory functions, and viewing the world through an intact optical apparatus. Thus we can observe how the fly's receptors respond when the fly sees something.

In this study we record signals generated by the photoreceptor and one class of first order interneurones, when the eye is exposed to a stimulus whose intensity is just sufficient to elicit a behavioural response. Previous behavioural experiments suggested that at or close to absolute threshold the individual photoreceptors receive approximately 10 photons per second (Fermi & Reichardt, 1963), and it has recently been shown that third order interneurones can respond to a single photon absorption (Lillywhite & Dvorak, 1980). However, recordings from receptors exposed to the original optomotor stimuli failed to detect responses to single photons (Scholes & Reichardt, 1969). We have repeated Scholes & Reichardt's experiment using improved intracellular recording techniques which now permit one to observe single photon signals (quantum bumps) in fly photoreceptors (Hardie, 1979). Our findings confirm that the fly is able to abstract the movement of its surroundings from a randomised pattern of discrete photon signals dispersed among many photoreceptors. We also describe processes of signal amplification and summation that could assist in this task.

METHODS

Animals. All experiments were performed on female *Musca domestica* taken from a laboratory culture.

Stimulus. The visual stimulus was a vertically oriented horizontally moving sinusoidal grating displayed on a CRT (Tektronix; P31 Phosphor) by an on-line laboratory computer (PDP11/03; Dvorak, Srinivasan & French, 1980). The spatial frequency used was 0·05 cycles/deg at the centre of the screen and the temporal frequency 1·2 cycles/sec. Contrast is defined as $(I_{max}-I_{min})/(I_{max}+I_{min})$ where I_{max} and I_{min} are the maximum and the minimum intensity of the grating respectively. The contrast of the grating was calibrated with a photodiode whose output

voltage was known to be linear with light. Care was taken to limit the area from which light could reach the photodiode to a small disk on the screen less than 0·5 cm in diameter. All contrasts were accurate to within 3%. The mean intensity was controlled by nine neutral density filters (Kodak Wratten gelatin filters) interposed between the screen and the eye, allowing coverage of an intensity range of approximately 7·7 log units in 0·1 log unit steps. The fly was placed 10 cm in front of the CRT screen, in the behavioural as well as the electrophysiological experiments. The resulting stimulus field was circular and covered a solid angle of 0·66 sr of the visual field of the animal.

Behaviour. In the behavioural experiments, the stimulus paradigm consisted of motion at constant speed towards the right for the first 80 s and then towards the left for another 80 s, with an abrupt reversal in between. The turning response evoked by the moving grating was measured in terms of the yaw torque (torque about the vertical axis) exerted by the tethered, flying animal (Fermi & Reichardt, 1963). The torque was measured as in Srinivasan & Bernard (1977). Yaw torques towards the right were reckoned as positive and those towards the left were reckoned as negative, and the turning response was measured as half the difference between the mean torques exerted during the last 60 s of right-motion and left-motion (the first 20 s of each phase were ignored to allow for transient changes in torque). The threshold stimulus for the turning response was arbitrarily defined as that for which the magnitude of the turning response is equal to the standard deviation of spontaneous fluctuations in torque.

Electrophysiology. The intracellular recordings were carried out using standard techniques (Hardie, 1979). For determining the mean bump rate in retinula and large monopolar cells (LMCs) a uniform screen of the same mean luminance as the grating was used as the visual input. The response was recorded on a chart recorder or occasionally on film. The records were analysed by eye because the variability of the amplitude of the bumps and the considerable amount of base line noise militated against an on-line computer analysis.

The signal-to-noise ratio in the receptor was defined with respect to the sinusoidal modulation of voltage set up by the stimulus and the accompanying noise. Signal amplitude was taken to be the standard deviation of the sinusoidal voltage response, determined by averaging the response to 100 cycles of stimulus presentation. The amplitude of noise was defined as the standard deviation of voltage fluctuations recorded from the receptor in response to a steady illumination of the same mean intensity as the sinusoidal stimulus. This was derived from 1000 points measured at 10 ms intervals.

Calibration of the stimulus screen. To derive the intensity of the stimulus in terms of number of photons available to each photoreceptor, we need to know the spectral distribution of the light emitted by the screen, the flux (power/cm^2) per steradian at the surface of the eye, the spectral and angular sensitivities of the cell, and the diameter of individual facets in the relevant region.

We measured the intensity and spectral composition of our source using a IL700 spectroradiometer (International Light, Massachusetts, U.S.A.) calibrated at the factory to 5% tolerance. The intensity of light emitted by the screen was measured with this instrument using a silicon detector (SEE 100F) placed where the fly's eyes would normally be, i.e. 10 cm in front of the screen, and the spectral distribution was obtained using a photomultiplier (IL PM 270D) together with a monochromator (IL 780). The intensity of light from the unfiltered screen was measured to be $(4{\cdot}6 \pm 0{\cdot}5) \times 10^{12}$ photons $\cdot$ s^{-1} $\cdot$ sr^{-1}, per cm^2 of detector surface (average $\pm$ S.D. of thirty measurements over a period of 10 days). The diameter of facets in the frontal eye regions of animals from which intracellular recordings (using the screen as light stimulus) were made was determined from flattened corneas to be 20 ± 2 μm. Consequently the quantal flux available to one ommatidium exposed to the unfiltered screen at a distance of 10 cm is $(1{\cdot}43 \pm 0{\cdot}27) \times 10^7$ photons $\cdot$ s^{-1} $\cdot$ sr^{-1}.

To compute the number of photons available to each cell, the photoreceptor's two dimensional angular sensitivity function has to be integrated. The angular sensitivity function was inferred from the spatial modulation transfer function to be a circular Gaussian of half width $\Delta\rho = 2{\cdot}3 \pm 0{\cdot}2°$, and the integral was calculated as

$$\int_{-\infty}^{+\infty}\int_{-\infty}^{+\infty} \exp\left[-\frac{4\ln 2}{\Delta\rho^2}\cdot(x^2+y^2)\right] dx\ dy = \frac{\Delta\rho^2\pi}{4\ln 2} = (1{\cdot}8 \pm 0{\cdot}33) \times 10^{-3} \text{ steradians}$$

Thus, $(2{\cdot}6 \pm 1{\cdot}0) \times 10^4$ photons $\cdot$ s^{-1} reach each R1-6 exposed to the mean luminance of the screen. The number of photons absorbed in each cell depends on the quantum efficiency.

We must also take account of the fact that the photoreceptors do not absorb photons of different wavelength equally readily. Fly photoreceptors of the type R1-6 have a double-peaked spectral

sensitivity function, with maxima in the U.V. and in the blue-green. Because our stimulus emitted negligible quantities of light at wave-lengths lower than 400 nm, only the long wave-length peak at 490 nm is of interest. In this region of the spectrum the spectral sensitivity curve of the cell, as determined electrophysiologically, closely follows the absorption spectrum of the rhodopsin found in these photoreceptors (Hamdorf, 1979). By convolving the spectral sensitivity for *Musca* R1-6 receptor cells, measured by Hardie (1979), with the measured spectral output of the screen, we found that the ratio between an equivalent flux of photons of peak wave-length and the photons emitted by the screen was 0·62. Consequently the unattenuated flux of the screen corresponds to $(1{\cdot}6 \pm 0{\cdot}6) \times 10^4$ photons of peak wave-length per second available to each R1-6 photoreceptor at the cornea.

Calibration of point source. The monochromatic light used in the point source experiment was focussed on one end of a light guide, the other end being fixed on a Cardan arm centred onto the animal. The light source subtended 44′ of the visual field of the fly. The wavelength used was 491 nm (optimum for R1-6) with a bandwidth of 9 nm. Using cut-off filters it was established that the energy transmitted by the side bands of the interference filter was less than 5% of the total energy. The light intensity was measured at 10 cm from the tip of the light guide with the IL 700 radiometer and three different detectors (Silicon detector: SEE 100F; vacuum photodiode: SEE 400D; photomultiplier: PM 270D; all International Light). All measurements were consistent to within 10%. The average intensity was $1{\cdot}2 \times 10^{-6}$ W or $2{\cdot}96 \times 10^{12}$ photons.s^{-1} per cm^2 of detector surface.

The flies used in the experiments involving a point source came from a different batch than the animals used in the experiments with the screen as stimulus, and were bigger and consequently had bigger facets. The facet diameter in the frontal region varied from 22 to 26 μm. For a point source of monochromatic light of peak wavelength the spectral and angular sensitivity function of the cells does not affect the number of photons available to the cell. Thus the average photon flux available to a cell when the point source is aligned with its optical axis is found to be $(1{\cdot}54 \pm 0{\cdot}23) \times 10^7$ photons.s^{-1} (without neutral density filters). All calibrations were checked using another radiometer of the same model as well as a Hewlett–Packard radiant flux meter (type 8330A). All measurements were consistent to within 10%.

RESULTS

Behavioural threshold

Fig. 1 depicts the behaviourally determined contrast sensitivity plotted against mean luminance over a 4 log unit intensity range. Contrast sensitivity is defined as the reciprocal of the contrast necessary to elicit the threshold turning response defined above. For a 100% modulated grating the average luminance for a threshold behavioural response was found to be 3·64 log units below the unattenuated mean luminance of the screen. Contrast sensitivity increases with luminance and, presumably, the over-all factor which limits detectability is the signal-to-noise ratio of the information received by the final stage of the movement detecting pathway. The interesting question of which part of the pathway is predominantly influencing this signal-to-noise ratio can only be answered by measuring this ratio at different levels of the detecting system. To start this investigation we made some preliminary measurements of the signal-to-noise ratio in retinula cells. The signal-to-noise in the retinula cells, as defined in Methods, increases with intensity over the whole range of intensities used. The implication of these observations will be discussed later (see Fig. 9 and Discussion).

Photoreceptor responses at behavioural threshold

Intracellular responses were recorded from 25 R1-6 cells, stimulated by the same uniform screen. Before collecting data from a cell, its physiological well being was

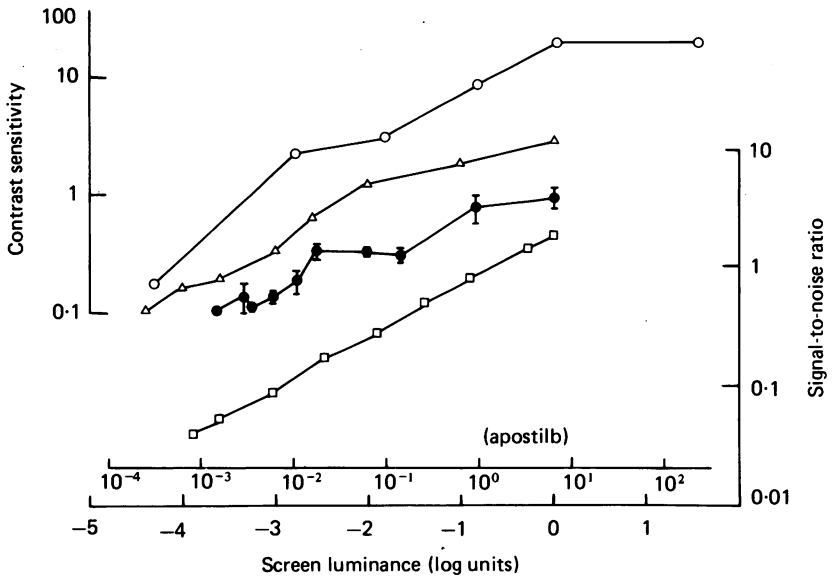

Fig. 1. Contrast sensitivity as a function of mean stimulus intensity in the fly *Musca domestica*. Behavioural results, obtained from the threshold of the optomotor turning response to a moving grating of low spatial wave-length, are compared with both the threshold of the H1 neurone, and with the signal-to-noise ratio in a photoreceptor under similar stimulus conditions. ●, behavioural data determined with our stimulus screen, using the standard grating of spatial frequency 0·05 cycles . deg^{-1} and temporal frequency 1·2 cycles . s^{-1}. Each data point represents the mean contrast sensitivity measured in four or more animals. Range bars show standard deviation. ○, comparable behavioural results of Fermi & Reichardt (1963) who used a vertically striped drum for a stimulus, with spatial frequency 0·02 cycles . deg^{-1} and temporal frequency 1·47 cycles . s^{-1}. Their luminance scale (apostilbs) was equated with our screen luminance using the calibrations described in the text. △, contrast sensitivity of a H1 neurone in the lobula plate of the fly *Lucilia sericata*, measured using our grating stimulus (D. R. Dvorak, unpublished data). □, The signal-to-noise ratio recorded intracellularly in a photoreceptor of type R1-6 while it was viewing our standard screen stimulus (signal-to-noise ratio is defined in the Methods section).

checked. Only those cells which produced a depolarizing receptor potential of more than 50 mV amplitude were analysed. Because the fly's eye is susceptible to defocussing by damage to the head capsule (Kirschfeld, 1972) the visual field of the cells was checked by measuring the modulation transfer function for spatially sinusoidal gratings over a frequency range of 0·012–0·6 cycles/deg. The half-width of the angular acceptance function $\Delta\rho$ (inferred by inverse transformation of the modulation transfer function) for the cells used lay between 2 and 2·5° when the eye was adapted to the maximum mean luminance of the screen. This range of values agrees well with the half-width of 2·5° measured from animals with intact optics (Scholes & Reichardt, 1969).

At low intensities the responses of photoreceptors consist of a train of fast discrete depolarizations, or 'bumps', superimposed upon a noisy background (Fig. 2*A*) (Hardie, 1979). The background noise increases when a dim light is turned on and

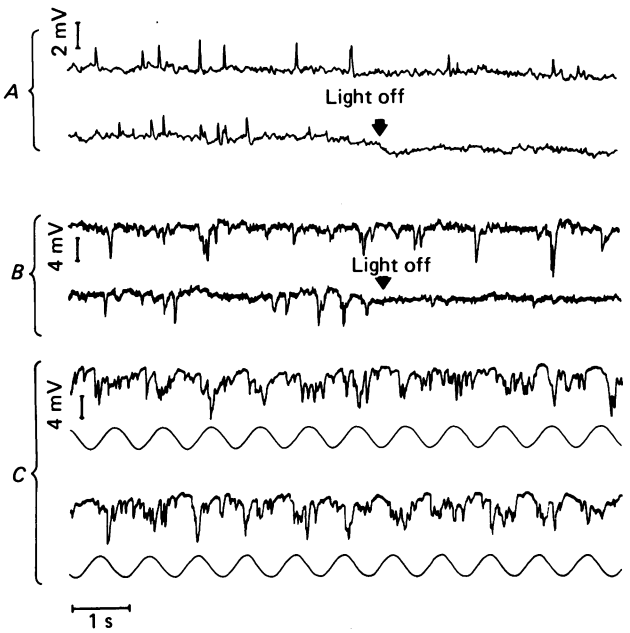

Fig. 2. The intracellular responses of a photoreceptor of type R1-6, and a first order interneurone (LMC) to our stimulus screen at intensities at, or below, the absolute threshold for the optomotor response. *A*, photoreceptor responses to a uniform screen with a luminance equal to the mean luminance of the grating stimulus at absolute threshold. The discrete depolarizations (bumps) are clearly seen. *B*, the response of an LMC to a screen luminance 1·2 log units below the absolute threshold value is a train of fast hyperpolarizing bumps. *C*, the response of an LMC to the standard grating of contrast 1 at the luminance corresponding to absolute threshold. The temporal modulation of the stimulus intensity at a corresponding point on the screen is shown below each trace. All records are from cells in the frontal eye region of female *Musca domestica*. The rising and falling phases of transient responses have been retouched for clarity.

in the best recordings slow, low amplitude bumps can be resolved in this noise in addition to the fast bumps. This phenomenon was further investigated and the results are described under the heading *Lateral interactions at low intensities.*

The following observations establish that these bumps are responses to single photon absorptions. (i) The bump rate is proportional to the stimulus intensity (Fig. 3). (ii) There are few dark bumps. (iii) The distribution of inter-bump intervals closely approximates an exponential function (Fig. 4*A*), suggesting that the train of bumps is governed by a Poisson process (Fuortes & Yeandle, 1964) with each bump corresponding to one absorbed photon (Lillywhite, 1977). The finding that about half as many bumps are produced as there are photons available to the cell (see *Photoreceptor quantum capture efficiency*) excludes the possibility of several photons being necessary to produce a bump.

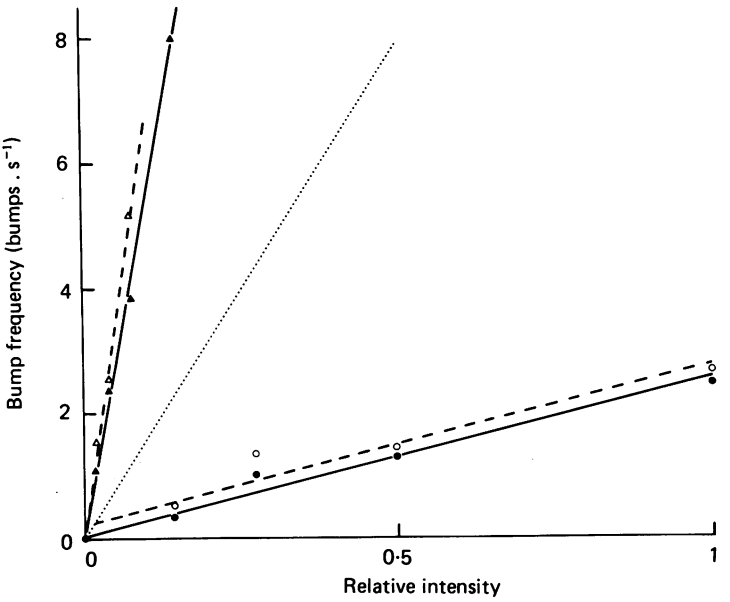

Fig. 3. The linear relationship between incident light intensity and bump frequency in two R1-6 (● and ○) and in two LMCs (▲ and △). Straight lines were fitted using linear regression analysis (regression coefficients were: ●, 0·989; ○, 0·969; ▲, 0·998 and △, 0·999). The CRT screen was the light source used in this experiment. As described in the text, the neural superposition theory predicts a ratio of six between lamina bumps and retina bumps at any given intensity (if each receptor bump produces a bump in the first order interneurone). The measured bump rates in the LMCs are approximately 3 times as high as the predicted values (dotted line).

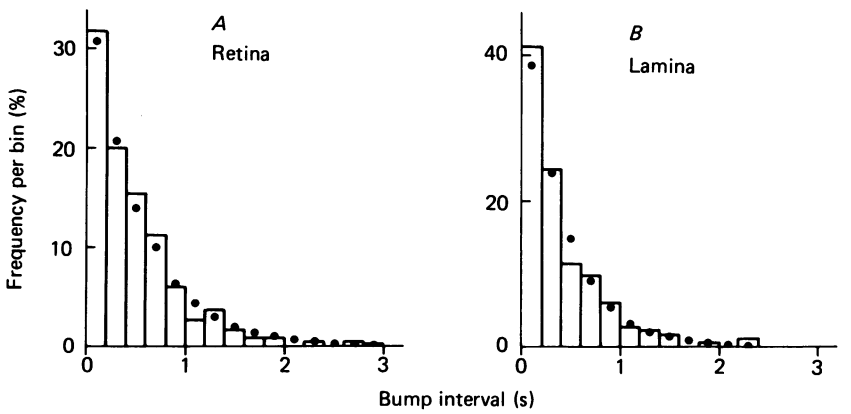

Fig. 4. A comparison between the measured intervals between the bumps recorded from photoreceptors in the retina (A; $n = 476$), and from first order interneurones in the lamina (B; $n = 185$). In both cases the measured distribution follows that predicted from a Poisson process with the same event rate (●). If a receptor bump triggered more than one lamina bump we would expect to see an excess of short intervals between lamina bumps.

To determine the bump rate at behavioural threshold we analysed over 2000 s of recordings from receptor cells subjected to the threshold stimulus. Bumps were discriminated by eye because of the variability of bump size (Fig. 5*A*) and the relatively poor signal-to-noise ratio. However, despite careful counting the error introduced by missing bumps buried in the noise must be significant and a large proportion of the variability in the results obtained in different cells could be due to this fact. The best recordings with low noise generally gave higher bump rates. This is consistent with the expectation that the bigger the noise, the more bumps are buried in it.

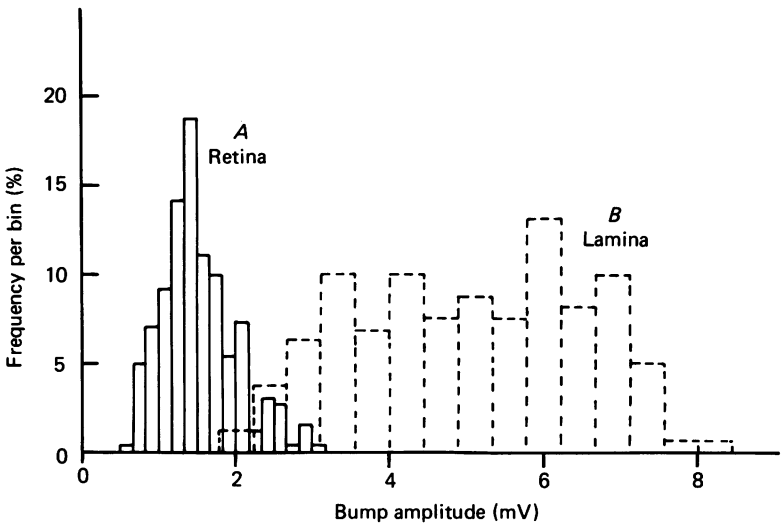

Fig. 5. The distribution of bump amplitudes recorded from (*A*) receptors R1-6 in the retina ($n = 260$) and (*B*) LMCs in the lamina ($n = 159$) when the retina was illuminated by the screen. Note that the bumps in the lamina are consistently larger than those in the retina.

The average bump rate at the threshold mean intensity for the behavioural response was found to be $1{\cdot}7 \pm 0{\cdot}7$ bumps . s^{-1} per cell (mean $\pm$ S.D.). This figure was obtained by averaging data acquired from twenty-five different retinula cells (all in the frontal, central region of the eye) after having corrected for the luminances of the screen at which the experiments for individual cells were carried out. The bump rate measured from each cell was given a weight proportional to the duration of the recording, so that, in effect, the pooled data was treated as one record.

The responses of first order interneurones at absolute threshold

We extended our study to the first order interneurones in the first optic ganglion, the lamina, by recording intracellularly the responses of the large monopolar cells (Zettler & Järvilehto, 1971; Laughlin & Hardie, 1978) to the screen. Recordings from LMCs were identified by a characteristically noisy base line in darkness, the highly sensitive triphasic response to a flash of light (Laughlin & Hardie, 1978) and the narrow angular sensitivity again obtained by inverse transformation of the modulation transfer function. Three questions were addressed: Does the response of LMCs to low light intensitities (which produce well separated bumps in the retina) show bumps?

Do these lamina bumps exhibit a linear relationship with the light intensity? Finally, what is the ratio between the number of retina and lamina bumps at a given intensity?

The position of the electrode was carefully chosen so as to record from the same frontal region in the lamina as we did in the retina. To further reduce the possible variability, recordings from the lamina and the retina were done on the same animal. Fig. 2*B* shows the response of a lamina cell to a uniform screen of luminance 1·2 log units below the mean value at absolute behavioural threshold. Fast hyperpolarizing bumps can be seen. Their maximum amplitude is as high as 8 mV, compared with 3 mV in the retinula cells (Fig. 5*A* and *B*). The frequency of inter-bump intervals predicted by Poisson statistics, under the assumption that each receptor bump produces only one bump in the lamina (● in Fig. 4*B*), is in good agreement with the experimental results (also Fig. 4*B*) and thus it is very unlikely that one retina bump produces more than one lamina bump.

Bump rates were measured in fifteen cells at six different light intensities, covering a range of approximately 1·5 log units, and the relationship between rate and intensity was linear (Fig. 3). Only very few dark bumps were observed in the dark-adapted lamina. At intensities producing more than 6–7 bumps.s^{-1} in the LMCs, it was difficult to measure bump rates accurately because a significant proportion of bumps tended to overlap or coincide. At the behavioural threshold the grating stimulus produces a distinct and continuous sinusoidal modulation of membrane potential in the LMCs (Fig. 2*C*). Using the linear relationship between the intensity of light and the bump rate in the lamina, the number of lamina bumps at the behavioural threshold can be calculated, by extrapolation, to be approximately 30 bumps.s^{-1}.

In the fly's neural superposition eye each of the LMCs is postsynaptic to six photoreceptors and although these receptors are located in different ommatidia they are aligned to share the same field of view (for review, see Kirschfeld, 1973). Given that each bump in a photoreceptor produces no more than one bump post-synaptically in the LMC, we would expect the interneurone bump rate to be at most 6 times that of the receptor under the same stimulus conditions. However, measurements of the bump rate in LMCs show that it is 18–20 times that of the receptor.

There are two possible explanations for an excess of bumps in interneurones. The first is that it is an artifact resulting from an underestimate of the receptors' true bump rate. The process of intracellular recording might damage receptors optically and lower their quantum capture efficiency, or bumps could be obscured by electrode noise. The surplus of interneurone bumps requires that we underestimate the true quantum catch of the receptor by a factor of three. Our calibrations (see Methods and below) show that an error of this magnitude is unlikely since, under our recording conditions, a receptor absorbs about half of the photons available to it at the cornea. The effect of any damage must be small, as indicated by the healthy responses and the apparently well focussed optics.

Many of the bumps seen in a single LMC must result from photons absorbed in receptors that lie outside the neural superposition projection of six cells. This convergence could be mediated either through coupling between receptors or through interneurones in the lamina. Further evidence for lateral interactions is presented below.

Photoreceptor quantum capture efficiency

At behavioural threshold (i.e. 3·64 log units below the unattenuated screen intensity) the photon flux available to the receptor is $(1{\cdot}6 \pm 0{\cdot}6) \times 10^4 \times 10^{-3{\cdot}64} = 3{\cdot}7 \pm 1{\cdot}4$ photons $\cdot s^{-1}$ (see Methods). The quantum capture efficiency (*QCE*) of photoreceptors of the type R1-6, is given by the ratio between the number of photons absorbed (i.e. the recorded bump rate) at the absolute behavioural threshold intensity ($1{\cdot}7 \pm 0{\cdot}7$) and the number of photons of optimum energy available in each cell at the same intensity ($3{\cdot}7 \pm 1{\cdot}4$). This gives $QCE = 0{\cdot}46$ ($\pm 0{\cdot}36$). The variability of over 70% in the *QCE* is partly due to the variability in the values of the anatomical parameters used in calculating the figure in the denominator of the *QCE*. We have assumed that the facet diameter and $\Delta\rho$ each vary by about 10%, a figure which includes measurement errors and real variations from facet to facet and cell to cell. High bump rates are probably measured in retinula cells with large facets and, or, big $\Delta\rho$ and thus the variability in *QCE* is certainly over-estimated. It is however impossible to obtain a quantitative estimate of the correlation between the variabilities of the two quantities involved in the calculation of the *QCE* from our data.

A more accurate estimate of the *QCE* can be obtained by using monochromatic light from a point source. If light of the optimum wavelength is used on-axis, only the facet diameter enters the calculations, and there is no need to assume the spectral sensitivity function or the angular sensitivity function of the retinula cell. Point source experiments also allow us to investigate the origin of the slow, low amplitude receptor bumps and of the excess bumps recorded from LMCs.

The average photon flux through one facet exposed to the monochromatic point source was calculated to be $(1{\cdot}54 \pm 0{\cdot}23) \times 10^7$ photons $\cdot s^{-1}$ (without neutral density filters) (see Methods). The light intensity was reduced by 6·8 log units and the response of R1-6 cells to this stimulus was observed. Fast depolarizations (Fig. 6*A*) were counted, and since the wave-length of the photons is optimum the *QCE* can directly be obtained by taking the ratio of bumps observed ($1{\cdot}1 \pm 0{\cdot}1$) to photons reaching one facet ($2{\cdot}1 \pm 0{\cdot}35$):

$$QCE = 0{\cdot}52\ (\pm 0{\cdot}14).$$

Thus, this more direct determination of the *QCE* using monochromatic light of optimal wave-length from a point source agrees quite well with the *QCE* of 0·46 determined using the extended light source.

There is however an interesting difference between the photoreceptors' responses to the point source and to the screen. With the extended source the response to very dim light was always composed of fast high-amplitude bumps but was accompanied by an increase in the background noise. In good recordings one could identify this noise as being composed of slower, smaller amplitude bumps. These small, slow bumps were not taken into account in determining the *QCE* because we initially believed that their origin was not in the cell being recorded from, but in the other 5 cells 'looking in the same direction' since these were shown recently by Shaw (1979) to be electrically coupled. However these slow events are practically absent if an on-axis point source is used (Fig. 6*A*). Consequently this coupling hypothesis has to be abandoned. To see if these small, slow amplitude events in receptors arise through lateral interactions in either the retina or the lamina we investigated the dependence of both receptor and LMC responses upon the position of a point source stimulus.

Lateral interactions at low intensities

If the small amplitude events recorded in one receptor arise from single photon signals in neighbouring cells then the frequency of small bumps should increase as a point source is moved away from the centre of a receptor's field of view. This is indeed the case. Off-axis light produces more small bumps and fewer large ones (Fig.

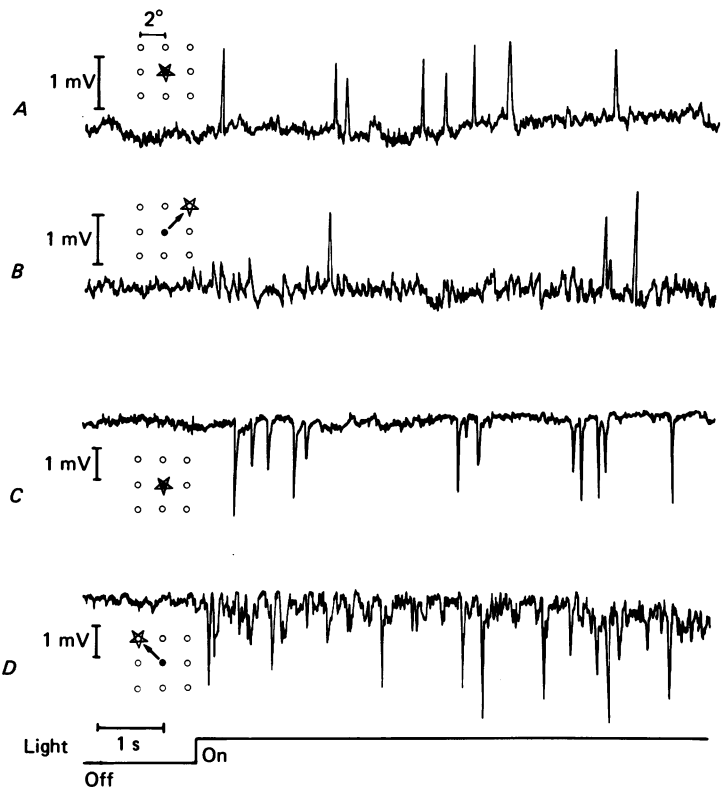

Fig. 6. Intracellular responses of a photoreceptor and an LMC to a monochromatic point source, showing the dependence of small bump frequency on stimulus position within the receptive field. *A*, retinula cell with *point source on-axis* and the light intensity attenuated by 6·8 log units. The response consists mainly of fast, high-amplitude bumps. *B*, same retinula cell immediately afterwards with *point source off-axis* in the position indicated in the inset and the light intensity 0·9 log units higher than before, so that the slow, low-amplitude bumps are more visible. *C*, lamina cell with *point source on-axis*. The light was attenuated by 7·8 log units of neutral density filters. Again, as in *A*, the response is a series of fast, high-amplitude bumps. *D*, same LMC immediately after recording *C*. The *point source* was positioned *off-axis* as indicated in the figure and the light intensity was increased by nearly two log units. Due to the higher light intensity, about the same number of direct, high-amplitude bumps are recorded in the LMC penetrated by the electrode but a very clear increase in low amplitude bumps can be observed.

6*A*,*B*). This effect was seen at eight off-axis positions of the stimulus but no attempt was made to map the dependence of small bump frequency on stimulus position, partly because the individual small bumps were difficult to resolve (Fig. 6*A*, *B*). We noticed that the 'noise' generated by superimposed small bumps increased to a

maximum at about 2° from the axis and then declined again at larger distances from the centre of the receptor's field. Since this angle corresponds to the spacing of receptors in the ommatidial mosaic this observation suggests that the interaction generating small bumps is greatest between neighbouring receptors. Our observation of a lateral interaction between receptors provides no evidence for the mechanism linking receptors. The interaction might be introduced by the electrode, if the penetration artifactually couples neighbouring cells in an ommatidium. This possibility can be tested by recording from monopolar cells which, since the electrode is now in the lamina, receive inputs from intact receptors.

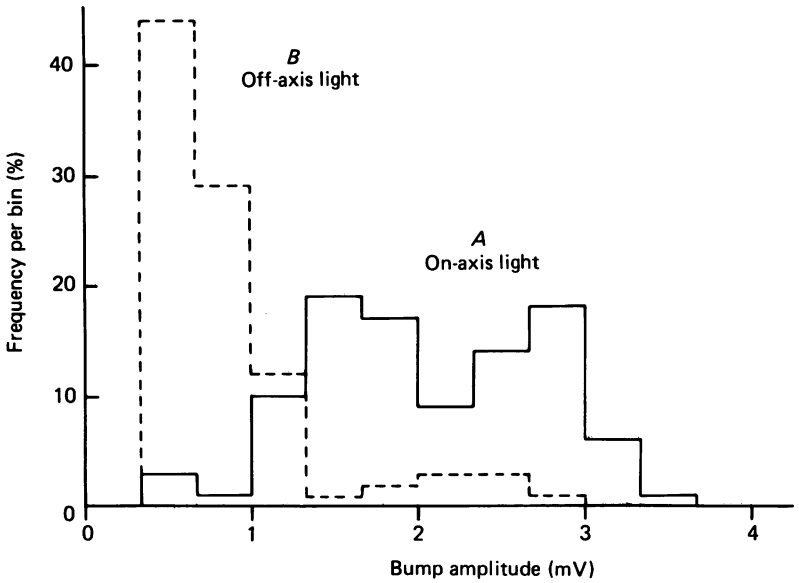

Fig. 7. Amplitude distributions for the bumps produced when an LMC is stimulated on-axis, in the centre of its visual field ($n = 77$) and off-axis, towards the periphery of the field ($n = 98$). Note that the relative frequencies of small and large bumps are dependent upon stimulus position.

As in the receptors, the LMC response changes with the position of a point source within its field of view. With the stimulus in the centre of the field, large hyperpolarizations occur with a frequency that is 6 times that observed in receptors under identical conditions. This is precisely the increase in frequency expected from the known projection of receptor axons to interneurones. By comparison, a point source in a more peripheral region of the field produces more events of a small amplitude (Fig. 6*C*, *D*; Fig. 7). These small events probably correspond to the small bumps seen in receptors under the same stimulus conditions and make it unlikely that the origin of small bumps in the receptors is artefactual.

The experiments using point stimuli have revealed a lateral summation of signals from receptors with different fields of view, and this interaction is seen as small bumps in both cell types. This summation is responsible for the large number of bumps seen in LMCs when an extended source was used (Fig. 3), since it was relatively easy to

distinguish between large and small bumps in receptors, but difficult in the LMCs. The small bumps in receptors are either too small to be resolved amidst electrode noise, or have a characteristic slow rising phase. With our recording equipment, display and time base, both large and small LMC bumps appear to have the same time course, and the amplification of signals at the insect visual system's first synapse (Shaw, 1968; Järvilehto & Zettler, 1971; Laughlin, 1973) apparently ensures that the small LMC bumps are large enough to be resolved against noise. Consequently, when using extended sources we counted only large bumps in receptors, but both small and large in LMCs. The similarity in time courses of large and small bumps in LMCs may reflect the limitations of our recording technique or the fact that during transfer from receptor to LMC, the high frequency components of the signal are selectively amplified (Järvilehto & Zettler, 1971). It is also possible that lateral interactions take place at the receptor terminals in the lamina, and that the slow bumps seen in the receptor cell body in the retina are smoothed and attenuated versions of the signal in its distal terminal. Our experiments do not allow us to isolate the level or levels in the visual pathway at which the lateral interaction takes place.

Comparison of behavioural contrast sensitivity with previous work

The results described above show in a direct manner that single photons producing well separated depolarizations in the receptor cells are an effective stimulus for the optomotor system in *Musca*. Scholes & Reichardt (1969) indirectly came to the same conclusion by estimating the light available to each retinula cell under the threshold condition from measurements of the light flux with a radiometer. Since extensive behavioural studies of the optomotor system in *Musca* have already been carried out (Fermi & Reichardt, 1963; Reichardt, Braitenberger & Weidel, 1968; Scholes & Reichardt, 1969) one would like to be able to compare our results with the previous studies. To enable this comparison the intensity of our light source relative to those of previous studies has to be established.

Two methods of calibration can be used: (i) the photon flux and the spectral distribution of light are measured using a radiometer and then compared with the corresponding measurements carried out by Scholes & Reichardt (1969); (ii) alternatively, the average response/intensity curve for the retinula cells in our experiments can be compared with the one published by Scholes & Reichardt (1969) and an identical response would then mean identical effective stimulus intensity. Scholes & Reichardt used both methods when they compared the screen intensity with the intensity of a point source. The comparison of response/intensity curves is more direct but it relies on the assumption that the cells are always equally sensitive. The two extreme response/intensity curves obtained in our experiments exhibit a shift of about 0·8 log units on the intensity scale, which is a considerable difference. Moreover, the fact that Scholes & Reichardt did not see any discrete bumps at low intensities while we did, also indicates that their cells had a lower sensitivity. Thus only the results obtained by the radiometric method (as described in Methods) were used to compare our results with the previous behavioural study of this species of fly.

The contrast sensitivity function of the optomotor response found by Fermi & Reichardt (1963) is plotted alongside our own in Fig. 1, after using our calibrations,

and those of Scholes & Reichardt (1969), to equate the intensity scales. Both sensitivity functions have the same shape but Fermi & Reichardt's sensitivities are consistently ten times greater than ours over the entire range of intensities we employed. This discrepancy is to be expected since Fermi & Reichardt (1963) used a rotating drum as their stimulus, and this subtended ten times the solid angle of our screen (5·5–6·9 sr, cf. 0·66 sr). Fermi & Reichardt also used a less conservative definition of behavioural threshold than our own.

DISCUSSION

We have correlated photoreceptor and first order interneurone responses with the absolute threshold for the optomotor response. This establishes the peripheral neural substrate for subsequent processing at threshold intensities. Previous experiments of this type, performed upon visual systems, have either looked at receptors alone (Scholes & Reichardt, 1969) or have recorded responses from an excised retina in which the normal circulation and optics were disrupted (Fain, Granda & Maxwell, 1977). In our physiological preparation, the retina and optics are virtually intact, and behavioural thresholds are determined with an intact animal. Consequently this invertebrate preparation is subject to far less uncertainty in its interpretation because, in both the behavioural and electrophysiological experiments, the retina is in virtually the same condition.

Our results confirm the conclusions drawn by Reichardt (1969) from behavioural experiments, namely that at the absolute-intensity threshold of the optomotor reflex the photoreceptors are responding with a random train of isolated single photon signals. As in other arthropod photoreceptors (Yeandle, 1958; Scholes, 1964) the single photon signals in photoreceptors are depolarizing quantum bumps. We find that the corresponding post-synaptic response of the first order interneurone, the LMC, is a hyperpolarizing bump. A comparison between photoreceptor and LMC bumps shows that single photon signals are useful signatures for exploring neural circuits. Synaptic amplification of signals, inferred from earlier experiments on LMCs (Zettler & Järvilehto, 1971), is confirmed by the observation that bumps are three times larger in LMCs than in photoreceptors. The sixfold increase in bump frequency seen when comparing LMCs and receptors viewing the same point source stimulus confirms the anatomical finding that six photoreceptors with the same field of view converge onto one set of post-synaptic interneurones (Kirschfeld, 1973). Thus the single photon signals, which occur randomly among different photoreceptors, allow one to separate the effects of synaptic amplification from convergency with a precision that was impossible when dealing with the highly correlated receptor responses observed at higher intensities (Laughlin, 1973). Moreover the single photon signals have demonstrated a new pathway for which, as yet, there is no satisfactory anatomical substrate. When using an extended source a comparison of photoreceptor and LMC bump rates shows that at least eighteen to twenty receptors converge onto each LMC and this indicates a significant lateral summation of photoreceptor responses. It is interesting to note that the previous experiments, conducted at higher intensities, showed that LMCs are subject to lateral inhibition (Zettler & Järvilehto, 1972; Mimura, 1976). This suggests that at low intensities the balance between lateral

inhibition and lateral summation tips in favour of summation. Indeed it is difficult to conceive of a function for lateral inhibition during the processing of discrete quantum bumps, whereas summation is an essential part of the acknowledged strategy whereby a visual system sacrifices spatial acuity for a workable signal-to-noise ratio at low intensities (Pirenne, 1967; Snyder, 1979).

The direct measurement of photoreceptor and interneurone responses reveals two factors which enable the fly's visual system to use single photon signals effectively and reliably. The first is that although the receptors produce a small quantum bump of 2 mV, the intrinsic receptor noise is comparatively small. This allows the second contributory factor, synaptic amplification to generate a well defined response of 2–8 mV amplitude, much larger than the receptor signal.

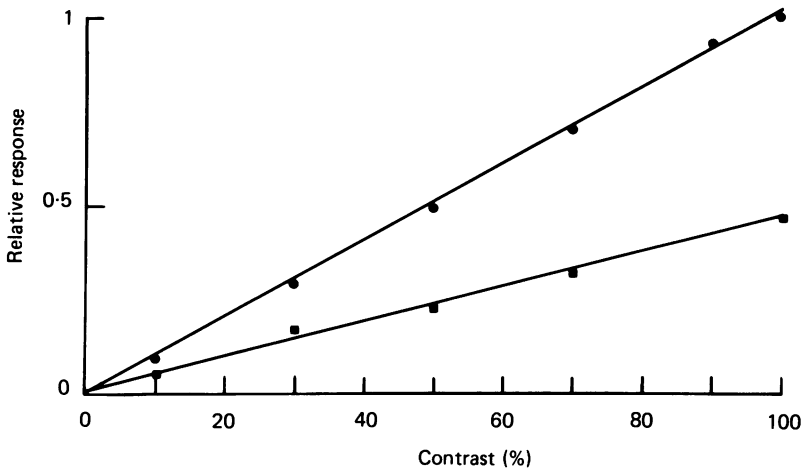

Fig. 8. Response amplitude as a function of stimulus contrast in a photoreceptor. The peak to peak amplitude, normalised relative to the maximum value obtained is plotted at two values of mean stimulus intensity, namely at screen intensity attenuations of 0·8 (●) and 1·6 (■) log units. In both cases the sinusoidal grating had a spatial frequency of 0·05 cycles.deg^{-1} and a temporal frequency of 1·2 cycles.s^{-1}.

As well as showing the amplitude of the smallest resolvable receptor response, the intracellular recordings provide a quantitative measure of the signal-to-noise ratio in receptors at threshold. This allows one to draw conclusions about the factors, both intrinsic and extrinsic, which contribute to the detectability of the stimulus. As a simple example we have compared the signal-to-noise ratios in receptors viewing threshold contrast modulations at a number of different mean intensities. A typical result is shown in Fig. 9. The data of Fig. 1 and the linear increase in signal amplitude with contrast at any of the mean intensities (Fig. 8) were used to calculate these values. The receptor signal-to-noise ratio at threshold declines with intensity. Since the signal-to-noise ratios of the behavioural responses under these conditions are constant (by definition) the fall in receptor signal-to-noise ratio can only mean that, for our stimulus, the visual system gets better at separating signal from noise as intensity falls. Because we used a slowly-moving, coarse grating this improvement in the resolution of the receptor inputs probably results from an increased spatial and

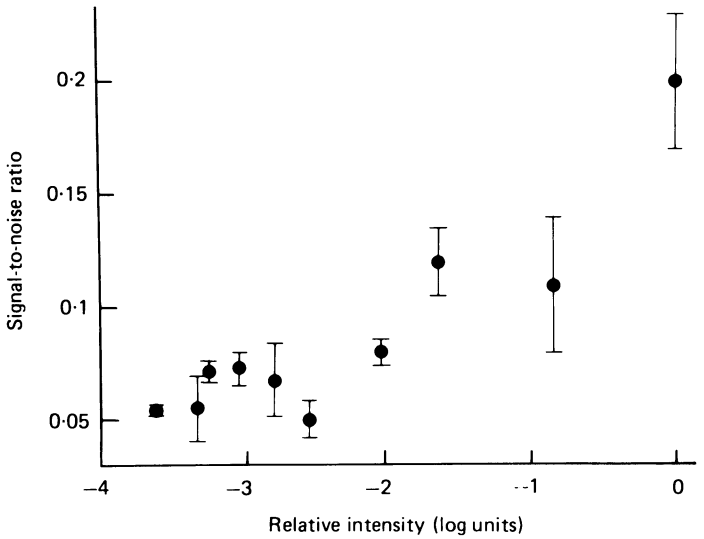

Fig. 9. Receptor signal-to-noise ratio (mean ± S.D.) at the behavioural threshold contrasts measured at a number of different intensities. The data presented in Fig. 1 was used together with the fact that the responses in R1-6 to sinusoidal gratings at any given intensity are found to be linear over the range of contrasts used (see Fig. 8). The intensity is measured relative to the unattenuated mean screen intensity.

temporal summation of receptor signals of the type inferred from analyses of the optomotor system's spatial resolving powers at low intensities (Dvorak & Snyder, 1978; Pick & Buchner, 1979; Srinivasan & Dvorak, 1980).

In conclusion, the analysis of single photon signals has revealed new pathways which have until now escaped notice, despite extensive anatomical and physiological studies of the fly's visual system. Our recordings also show that it is possible to examine the role of the first order interneurones L1 and L2 in determining the optomotor threshold, presuming that they feed into the optomotor system. Thus the correlation of neural responses with behaviour can take what were previously abstract measures of receptor and interneurone responses, and place them within the context of the discriminatory tasks necessary for vision.

We wish to thank Steve Shaw, Richard Payne and David Williams for their suggestions and critical comments on the manuscript.

REFERENCES

DeVoe, R. D. & Ockleford, E. M. (1976). Intracellular responses from cells of the medulla of the fly *Calliphora erythrocephala*. *Biol. Cybern.* **23**, 13–24.

Dvorak, D. R., Bishop, L. G. & Eckert, H. E. (1975). On the identification of movement detectors in the fly optic lobe. *J. comp. Physiol.* **100**, 5–23.

Dvorak, D. R. & Snyder, A. W. (1978). The relationship between visual acuity and illumination in the fly *Lucilia sericata*. *Z. Naturf.* **33c**, 139–143.

DVORAK, D. R., SRINIVASAN, M. V. & FRENCH, A. S. (1980). The contrast sensitivity of fly movement-detecting neurons. *Vision Res.* **20**, 397–407.

FAIN, G. L., GRANDA, A. M. & MAXWELL, J. H. (1977). Voltage signal of photoreceptors at visual threshold. *Nature, Lond.* **265**, 181–183.

FERMI, G. & REICHARDT, W. (1963). Optomotorische Reaktionen der Fliege *Musca domestica*. *Kybernetik* **2**, 15–28.

FUORTES, M. G. F. & YEANDLE, S. (1964). Probability of occurrence of discrete potential waves in the eye of *Limulus*. *J. gen. Physiol.* **47**, 443–463.

HAMDORF, K. (1979). The physiology of invertebrate visual pigments. In *Handbook of Sensory Physiology*, vol. VII/6a, ed. AUTRUM, H., Berlin: Springer.

HARDIE, R. C. (1979). Electrophysiological analysis of fly retina. I. Comparative properties of R1-6 and R7 and 8. *J. comp. Physiol.* **129**, 19–33.

HAUSEN, K. (1976). Functional characterization and anatomical identification of motion sensitive neurons in the lobula plate of the blowfly *Calliphora erythrocephala*. *Z. Naturf.* **31c**, 629–633.

JÄRVILEHTO, M. & ZETTLER, F. (1971). Localized intracellular potentials from pre- and postsynaptic components in the external plexiform layer of an insect retina. *Z. vergl. Physiol.* **75**, 422–440.

KIRSCHFELD, K. (1972). The visual system of *Musca*: studies on optics, structure and function. In *Information Processing in the Visual Systems* of Arthropods, ed. WEHNER, R., pp. 61–74. Berlin: Springer.

KIRSCHFELD, K. (1973). Das neurale Superpositionsauge. *Fortschr. Zool.* **21**, 229–257.

KIRSCHFELD, K., FRANCESCHINI, N. & MINKE, B. (1977). Evidence for a sensitising pigment in fly photoreceptors. *Nature*, Lond. **269**, 386–390.

LAND, M. F. (1977). Visually guided movements in invertebrates. In *Function and Formation of Neural Systems*, ed. STENT, G. S. Berlin: Dahlem Konferenzen.

LAUGHLIN, S. B. (1973). Neural integration in the first optic neuropile of dragonflies. I. Signal amplification in dark adapted second order neurons. *J. comp. Physiol.* **84**, 335–355.

LAUGHLIN, S. B. & HARDIE, R. C. (1978). Common strategies for light adaptation in the peripheral visual systems of the fly and dragonfly. *J. comp. Physiol.* **128**, 319–340.

LILLYWHITE, P. G. (1977). Single photon signals and transduction in an insect eye. *J. comp. Physiol.* **122**, 189–200.

LILLYWHITE, P. G. & DVORAK, D. R. (1981). Responses to single photons in a fly optomotor neurone. *Vision Res.* **21**, 279–290.

MIMURA, K. (1976). Some spatial properties in the first ganglion of the fly. *J. comp. Physiol.* **105**, 65–82.

PICK, B. & BUCHNER, E. (1979). Visual movement detection under light- and dark adaptation in the fly, *Musca domestica*. *J. comp. Physiol.* **134**, 45–54.

PIRENNE, M. H. (1967). *Vision and the Eye*, 2nd edn., pp. 141–152. London: Chapman and Hall.

REICHARDT, W. (1970). The insect eye as a model for analysis of uptake transduction and processing of optical data in the nervous system. In *The Neurosciences, Second Study Programme*, ed. SCHMITT, F. O. New York: Rockefeller University.

REICHARDT, W., BRAITENBERG, V. & WEIDEL, G. (1968). Auslösung von Elementarprozessen durch einzelne Lichtquanten im Fliegenauge. *Kybernetik* **5**, 148–170.

SCHOLES, J. H. (1964). Discrete subthreshold potentials from the dimly lit insect eye. *Nature, Lond.* **202**, 572–573.

SCHOLES, J. H. & REICHARDT, W. (1969). The quantal content of optomotor stimuli and the electrical responses of receptors in the compound eye of the fly *Musca*. *Kybernetik* **6**, 74–80.

SHAW, S. R. (1968). Organization of the *Locust* retina. *Symp. zool. Soc. Lond.* **23**, 135–163.

SHAW, S. R. (1979). Photoreceptor interaction of the lamina synapse of the fly's compound eye. *Investive. Ophth.* **18**, (suppl.), 6.

SNYDER, A. W. (1979). Physics of vision in compound eyes. In *Handbook of Sensory Physiology*, vol. VII/6a, ed. AUTRUM, H. Berlin: Springer.

SRINIVASAN, M. V. & BERNARD, G. D. (1977). The fly can discriminate movement at signal/noise ratios as low as one-eighth. *Vision Res.* **17**, 609–616.

SRINIVASAN, M. V., DVORAK, D. R. (1980). Spatial processing of visual information in the movement-detecting pathway of the fly. *J. comp. Physiol.* **140**, 1–23.

STRAUSFELD, N. J. (1976*a*). Mosaic organisations, layers, and visual pathways in the insect brain. In *Neural Principles in Vision*, ed. ZETTLER, F. & WEILER, R. Berlin: Springer.

STRAUSFELD, N. J. (1976*b*). *Atlas of an Insect Brain*. Berlin: Springer.

YEANDLE, S. (1958). Evidence of quantized slow potentials in the eye of *Limulus*. *Am. J. Opthal.* **46**, 82–87.

ZETTLER, F. & JÄRVILEHTO, M. (1971). Decrement-free conduction of graded potentials along the axon of a monopolar neuron. *Z. vergl. Physiol.* **75**, 402–421.

ZETTLER, F. & JÄRVILEHTO, M. (1972). Lateral inhibition in an insect eye. *Z. vergl. Physiol.* **76**, 233–244.

ZETTLER, F. & JÄRVILEHTO, M. (1973). Active and passive axonal propagation of non-spike signals in the retina of *Calliphora*. *J. comp. Physiol.* **85**, 89–104.